Numerical simulations of the impact of the 20 March 2015 eclipse on UK weather

Article

Accepted Version

PHILOSOPHICAL TRANSACTIONS A

rsta.royalsocietypublishing.org

Research

Article submitted to journal

Subject Areas:
Meteorology

Keywords:
Eclipse, Boundary-Layer

Author for correspondence:
P.A. Clark
e-mail: p.clark@reading.ac.uk

Numerical Simulations of the Impact of the 20 March 2015 eclipse on UK Weather

P.A. Clark[1]

[1]Department of Meteorology, University of Reading.

Short lead-time forecasts using the operational United Kingdom Variable-Resolution ('UKV') configuration of the Met Office's Numerical Weather Prediction model, with horizontal grid-length 1.5 km over the UK, with and without a representation of the 20 March 2015 eclipse, has been used to simulate the impact of the eclipse on UK weather. The major impact was surface-driven through changes to surface heat and moisture fluxes which changed the boundary-layer development. In cloud-free areas, the nocturnal stable boundary-layer persisted or quickly re-established during the eclipse. Surface temperatures were reduced by 7-8 °C, near-surface air temperature by 1-3 °C, near-surface winds were backed, typically by 20 °. Impacts on wind speed were small and variable and would have been very difficult to detect.

Smaller impacts occurred beneath cloud. However, the impact was enhanced because most of incoming radiation which reached the surface was driving surface sensible heat flux rather than moisture flux, and the near surface air temperature impact (0.5-1 °C) agrees reasonably well with observations.

The modelled impact of the eclipse was substantially reduced in urban areas due to their large thermal inertia. Experience from other assessments of the model suggests that this lack of response may be exaggerated.

Surface impacts propagated upwards and down stream with time, resulting in a complex pattern of response, though generally near-surface temperature differences persisted for many hours after the eclipse. The impact on atmospheric pressure fields was insufficient to account for any significant perturbations to the wind field when compared with the direct impacts of surface stress and boundary-layer mixing.

THE ROYAL SOCIETY PUBLISHING

1. Introduction

Meteorological flows are driven by incoming solar radiation which varies over a wide range of time scales. One of the shortest modes of variability is that due to solar eclipses. Though the evening and morning transitions have similarly short timescales, they occur in the context of the diurnal cycle of solar radiation. Though each is unique in itself, and occurs in a unique meteorological context, some generic features have been proposed associated with eclipses. Clayton (1901) [1] was the first to deduce wind and temperature changes, during the 28 May 1900 solar eclipse and a number of subsequent studies were reviewed by Aplin and Harrison (2003) [2].

Any such study requires the establishment of an estimate of what would have been observed had the eclipse not happened. This is made quite difficult by the natural variability of the weather, and no single approach is perfect. Some form of time-interpolation may be used [3–5] but it is difficult to be certain when the eclipse impact finishes. The advent of detailed Numerical Weather Prediction (NWP) models provides an alternative background in the form of a (short) forecast from an analysis prior to the eclipse first contact. This approach has been used, for example, to evaluate the impact of the 11 August 1999 eclipse [6], but is limited by the accuracy of predictions of the local conditions by the forecast model.

Given this approach, it is worth asking the question 'what impact would the NWP model have predicted?', thus enabling a completely clean comparison to be made, albeit of model-predicted impact. This approach was taken by Prenosil (2000) [7] to study the 11 August 1999 eclipse, but using a relatively coarse-resolution model (with horizontal grid spacing about 65 km) which would be incapable of representing small-scale effects, especially due to cloud and topography. Over the last decade, so-called convective-scale or convection permitting models have become operational, capable of representing much local detail with some accuracy [8]. In this study, the operational 'UKV' configuration of the Met Office's NWP model, with horizontal grid-length 1.5 km over the UK, is used to simulate the impact of the 20 March 2015 eclipse on a short forecast of UK weather.

The models which form the basis of weather-forecasting and climate-prediction systems are complex numerical simulations of the many contributing processes. At their core is a numerical solution of the fluid-dynamics of the atmosphere, but in addition the models need to compute the impact of unresolved turbulence, the formation and dissipation of clouds and precipitation, the interaction of electromagnetic radiation with gases in the air and with clouds, and interaction with the sea- and land-surface (which, itself, needs a treatment of the sub-surface).

We can only properly test these models by comparison with the real system. However, the earth system is believed to be a chaotic system which never repeats itself. The occurrence of a predictable perturbation of the system provides a unique opportunity to test the system. In this case, the response to a short time scale, large amplitude perturbation to the incoming solar radiation may be tested. Comparison with observations provides some measure of confidence in the model (and *vice versa*!), but also helps inform choices when analysing the observations (e.g. does the air temperature recover quickly after the eclipse, or do impacts persist?). Furthermore, since we have full, high time-frequency fields available, we can evaluate impacts that are extremely difficult to observe.

2. Model Configuration

(a) Description of MetUM configuration

The results presented here make use of precisely the configuration of forecast models used by the Met Office on the day of the eclipse. The forecast is based on version 9.0 of the Met Office's Unified Model (MetUM). This uses a semi-Lagrangian, semi-implicit solution to the deep-atmosphere, non-hydrostatic equations [9,10]. The model runs on a rotated latitude/longitude horizontal

grid with Arakawa C staggering, and a terrain-following hybrid-height vertical coordinate with Charney-Philips staggering. The model includes a comprehensive set of parametrizations, including surface [11], boundary layer [12], and convection [13] (with additional downdraught and momentum transport parametrizations), though for the high-resolution runs presented here the convection scheme was not used. The standard mixed-phase cloud micro-physics [14] has been extensively modified to include more prognostic variables. Up to six bulk moisture variables can be used (vapour, cloud water, rain water, ice crystals, snow and graupel), with a single moment (the mixing ratio) describing each. However, various options have been implemented to allow diagnostic treatment of some variables. The precise configuration is designated in the Met Office as 'Parallel Suite 35' (PS35), which includes a new dynamical core (ENDGAME) based upon iterative solution, and a 'blended' version of the boundary-layer scheme (in the high-resolution model), the main impact of which, at these resolutions, is to use horizontal mixing based upon that diagnosed in the vertical direction within the boundary layer.

The boundary-layer scheme [12] is of particular importance for the eclipse impact. The scheme is a first-order scheme which diagnoses the boundary layer as being one of several distinct types (stable, shear-driven, convective, well-mixed (possibly strato-cumulus-covered), cumulus-capped, decoupled strato-cumulus, cumulus below decoupled strato-cumulus) and, for each type, derives a flux profile which may include locally driven fluxes based upon the gradient and non-locally driven fluxes derived from teh surface or cloud top. It has been shown to work well especially for cloudy boundary layers.

The forecast is produced from a nested configuration. A global configuration, with a horizontal grid length approximately 17 km at mid-latitudes and 70 vertical levels (with top level at about 80 km), is run every 6 h, using an analysis made using 4-dimensional variational assimilation [15] nominally at 0000, 0600, 1200 and 1800 UTC. This provides lateral boundary conditions for the high-resolution 'UKV' configuration. This configuration is designed specifically for UK forecasting. It uses variable horizontal resolution, with resolution approximately 1.5 km over the UK, stretching to 4 km at the boundaries. Figures in this paper are plotted (at most) just over the area with 1.5 km resolution. The UKV configuration also has a different set of 70 vertical levels from, and a lower 'top' than the global configuration (40 km), resulting in much higher resolution in the boundary layer. A UKV analysis is produced every 3 h, using 3-dimensional variational assimilation [16], but forecasts are only run from the 0300, 0900, 1500 and 2100 UTC analyses.

Results reported here are taken from runs started using the 03 UTC analysis. This choice represents a compromise which experience suggests is close to optimal. The objective is not to assess the ability of the model to predict the weather. The forecast system is routinely verified against observations as a part of the operational use of the model, and one case would add nothing to this evaluation. The objective is to estimate the impact of the eclipse on local weather. This assessment is subject to error. The error arises from errors in the model state and errors in the model formulation. To minimise the former, the model state as close to analysis as possible should be used (though this is not perfect!). The experiments could have been run from the 06 UTC analysis but this might have still been affected by 'spin-up' from the analysis system (which uses a nudging method to introduce analysis increments up to 0700). In practice, there was very little difference between the 0300 3h forecast and the 0600 analysis. The choice of lateral boundary condition is of minor importance for the short forecast presented. The experiments could have used time-interpolated global analyses (so-called 'dynamical adaptation') but the 0600 global analysis would have then been inconsistent with the 0600 UKV analysis (which is operationally run before the global forecast), and the coarse time interpolation may have introduced errors in the form of gravity waves which might have propagated into the interior. The size of the domain is such that small changes in lateral boundary conditions would have very little impact on the UK area in the less than 9-hour period studied. As noted below, the same lateral boundary conditions were used with and without the eclipse.

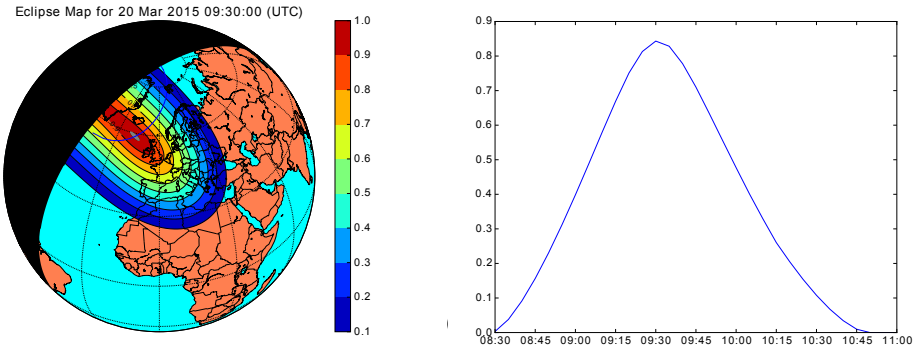

Figure 1. (a) Computed eclipse shadow factor at 0930 UTC, 20/03/2015. The grey central region is the area of total eclipse. The blue line shows the path of totality. (b) Eclipse factor at Reading plotted every 5 min.

(b) Description of calculation of eclipse impact

The calculation of the impact of the eclipse, while a routine astronomical calculation, is relatively complex if performed with a high degree of accuracy. Rather than try to reproduce this calculation, the data provided by NASA [17] were used. These provide the location, path width, and moon:sun diameter ratio for the total eclipse (amongst other things), at two-minute intervals. From this it is relatively straightforward (assuming a spherical earth, as in the MetUM) to estimate an apparent angular separation of the moon and sun observed from any location on earth. From this, a reduction in incoming solar radiation was estimated on the basis of overlapping circles. Some extrapolation of the apparent moon position was also required during the times before and after totality, though the impact of these is not large.

The procedure as a whole is not perfect, and further complicated by the fact that the model uses a spherical earth approximation, but differences between the calculated reduction in incoming radiation and the eclipse magnitude published by NASA [17] are of order 1%. The calculated 'eclipse shadow factor' (i.e. the proportional reduction in top of atmosphere incoming radiation) at 0930 UTC (approximately the time of maximum eclipse over central England) is shown in Fig. 1(a), while the time series of the factor at Reading is plotted (at 5-minute intervals) in Fig. 1(b). This has a peak of about 84%, compared with the accurate figure of 85%. Reading is shown purely as a example - the curve varies very little over most of England.

The radiation scheme in the MetUM is that of Edwards and Slingo [18]. It is a comprehensive code that calculates short-wave (SW) and long-wave (LW) interaction with the atmosphere and surface. It is a computationally expensive code, and the full code is only called every 15 minutes, with an approximate update due to changes in cloud every 5 minutes. The direct SW is updated for change in solar declination every time step (1 minute).

Two runs of the model were performed; the first was the 'standard' run, as per the operational forecast, without any allowance for the eclipse. In the second, the geographially-varying calculated eclipse shadow factor was applied to this direct incoming SW radiation every time step within the radiation code.

Only the UK model had this factor applied; though the shadow clearly extends outside the UKV area, most of the boundary is over the sea, where the actual meteorological impact is expected to be very small (and the modelled impact even smaller, for reasons explained below). Therefore, the operational global boundary conditions were used to drive the UKV with and without the impact of the eclipse.

Note that the author worked with Met Office staff to implement a similar simulation to provide a real-time forecast. The algorithm used here has been improved compared with that used on the

day; while the overall conclusions are not different, the results presented here differ in detail from the forecasts issued on the day.

3. Synoptic background

On 20 March 2015 a high pressure area was centred to the west of Ireland, and the UK was experiencing a weak pressure gradient, with a weak north-westerly wind over the northern half of the country bringing a weak cold front, comprising mainly broken cloud and little or no precipitation. Ahead of this was a cloud-free region which covered central and SW England and Wales during the eclipse. This was bounded by a region over SE England and East Anglia with weak north-easterly to easterly flow.

Figure 2 shows an image from the Meteosat Second Generation satellite at 1000 UTC. This indicates the temperature of the cloud top or surface where there is no cloud. Lighter shades are colder and hence higher. The figure shows extensive low cloud over much of the UK, with the clear band evident and a very narrow band of mid-level cloud on its southern edge.

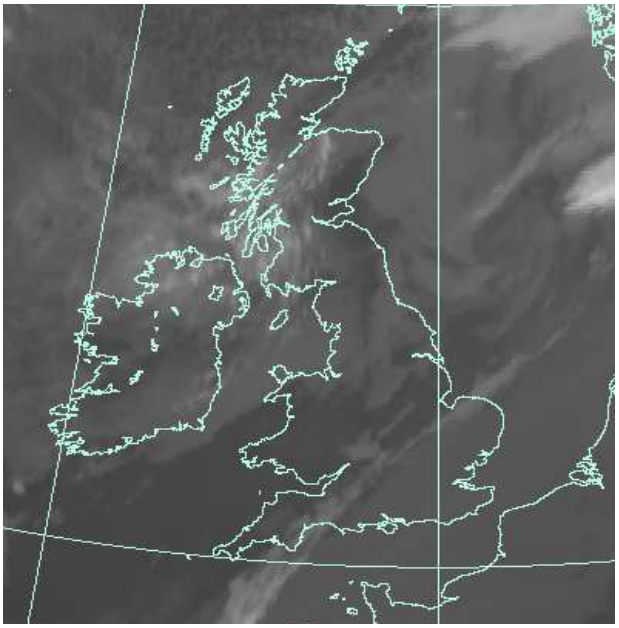

Figure 2. Infra-red image from the Meteosat Second Generation satellite at 1000 UTC showing cloud cover (data courtesy EUMETSAT).

4. Model Results

(a) Near-surface weather

In general, incoming SW radiation has the greatest meteorological impact in cloud-free regions, where it primarily warms the surface and thence, largely through turbulent surface exchange, the lowest layer of the atmosphere known as the boundary layer. Cloud has a high SW albedo, though some SW is usually transmitted and a little absorbed. Figure 3 shows the modelled fractional low- and medium- level cloud cover for comparison with Fig. 2. There was no significant high-level cloud. The model cloud distribution is not perfect, especially in detail, but the gap over central and south west England and Wales is well captured, along with the band of mid-level cloud to

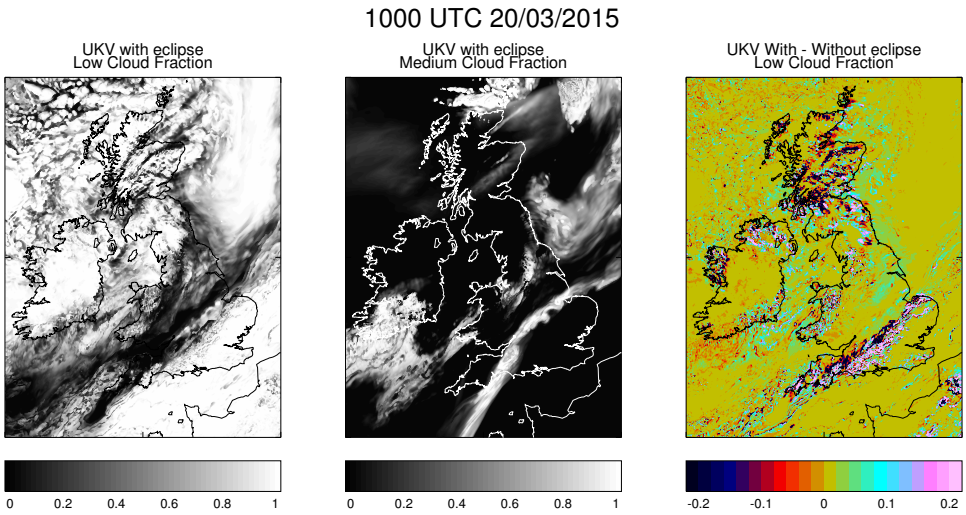

Figure 3. Modelled low cloud cover (left) and medium cloud cover (centre) 1000 UTC, with eclipse included. The difference in low cloud is shown right.

the south of it. The low-level cloud over south-east England is perhaps a little more fragmented at the NW edge in the model, though the satellite image is of too low resolution to see this in detail. The model also seems to have a too much low cloud over Wales.

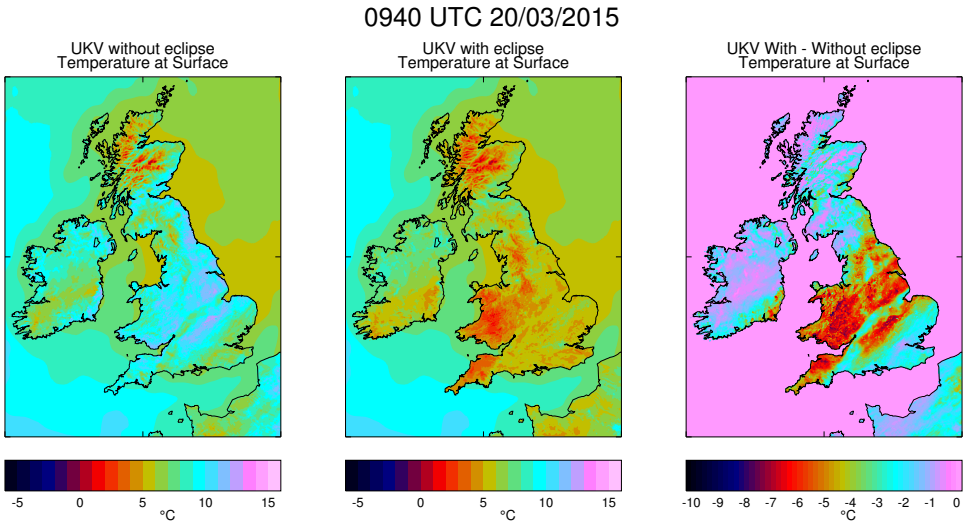

Figure 4. Map of surface (skin) temperature at 0940 UTC, left to right, without eclipse, with eclipse and difference.

The land surface skin temperature is fast to respond to changes in incoming SW. Figure 4 shows the surface temperature at 0940, very shortly after maximum eclipse and close to the maximum impact of surface SW. The broad band with little or no cloud cover has a maximum relative cooling of 7-8 °C. Areas with 100% cloud cover generally show less than a degree reduction, with the exception of the band running through Suffolk, Surrey and Sussex, which has a 2-3 °C reduction.

Note that the impact over the sea is identically zero. This is a simplification of the operational forecast model. The diurnal cycle of sea surface temperature (SST) is generally much smaller than that over land under clear skies. This is because the land surface is opaque, so incoming SW only heats a very thin 'skin' at the surface. Heat can then only be transmitted to the sub-surface through diffusive conduction. In contrast, SW penetrates to a significant depth (of order 1 m), so heats a substantial volume of water. Furthermore, while the surface heating generally makes the water less dense than that beneath, nocturnal surface cooling can result in convective overturning, so at dawn the near surface is usually quite well-mixed. We would expect the heating of the sea surface during the first few hours of the day to be only a small fraction of a degree. However, because of the small observed daily cycle, the approximation is made in the model that the SST does not change at all during a forecast. Thus, while the impact on SST of the eclipse is expected to be very small, the model used is incapable of predicting it. It should be noted that work is currently under way to couple the UKV model with the operational 'shelf seas' model, in part to overcome this limitation, so in future it may be possible to confirm this assumption.

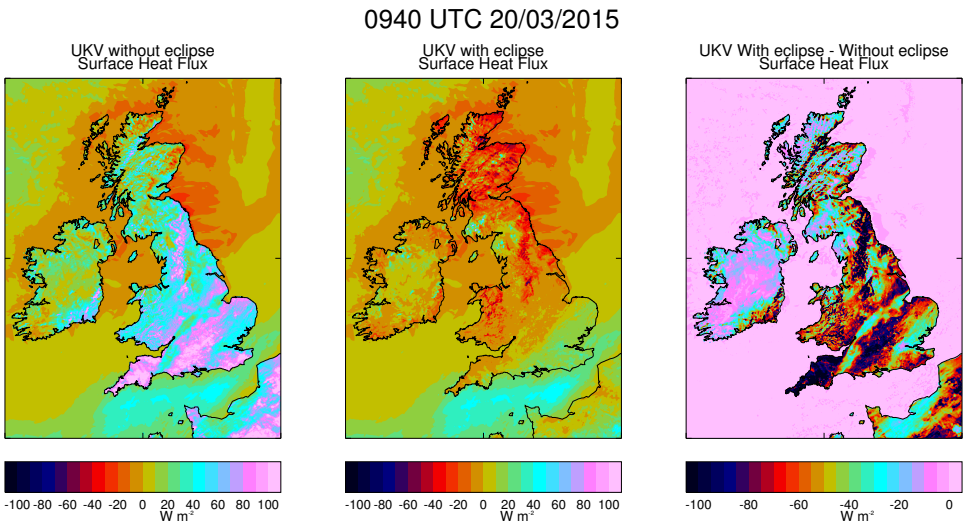

Figure 5. Modelled surface sensible heat flux at 0940 UTC, without eclipse included (left), with (centre) and difference (right).

Figure 5 shows the impact of the eclipse on surface sensible heat flux (at 1000 UTC). Over land, there is a reduction of up to 100 W m^{-2} under clear skies, similar under regions with 100% but relatively thin or broken cloud cover, and even 20-30 W m^{-2} under thicker total cloud. Over parts of Northern England and Scotland, especially on the eastern side of orography, the sensible heat flux actually changes sign due to the eclipse, becoming weakly stable rather than weakly unstable.

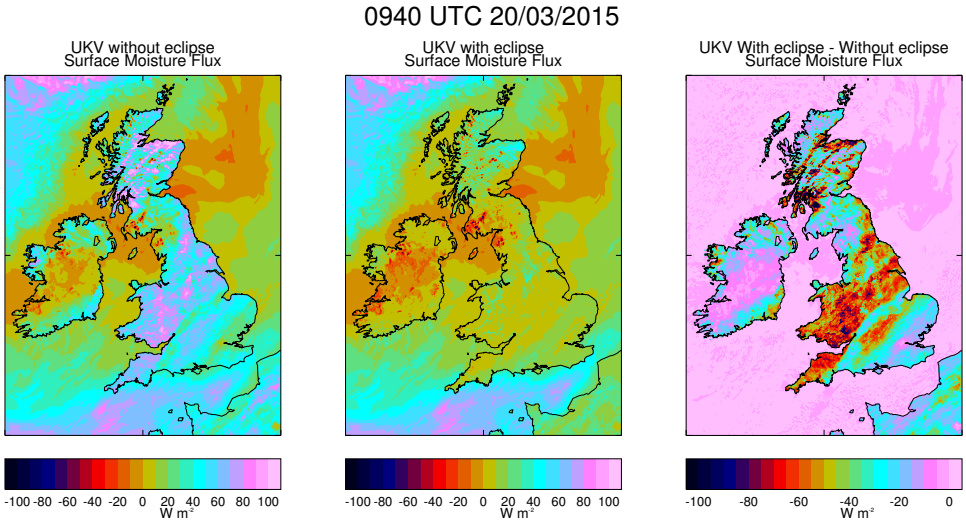

Figure 6. Modelled surface latent heat flux at 0940 UTC, without eclipse included (left), with (centre) and difference (right).

This is not, however, the whole story. Figure 6 shows a similar reduction in latent heat flux (through evaporation of surface water and plant evapotranspiration) in clear-sky areas, 20-30 W m^{-2} under thinner cloud and up to 10 W m^{-2} under thick cloud. Thus, under a clear sky roughly half the surface heat flux would have been latent, while under cloud the proportion of latent flux is less, especially under thicker cover. Hence, the contrast in sensible heat flux between clear-sky and cloud is less than might have been expected from changes in incoming SW alone.

The smaller relative impact on latent heat flux below cloud reflects the higher near-surface relative humidity, which reduces the surface/air humidity gradient. The result is that there is a smaller difference in impact on near-surface air temperature between clear skies and cloudy than might have been expected from changes in incoming radiation alone. The near-surface air is conventionally measured at the height of a Stevenson screen, in the UK nominally 1.25 m. The impact of the eclipse on the 1.25 m temperature at 0940 is shown in Fig. 7. This is generally the time of largest impact, though the difference at 1000 UTC is not much less. Cloud-free areas show deficits approaching 4 °C over Wales and parts of central England, though the norm is closer to 2-3 °C. Only under the thickest cloud is the deficit close to zero, with 1 °C typical under thinner or broken cloud.

Comparison with observations raises a number of issues. Those associated with imperfect initial and boundary conditions for the model have been discussed above. However, the model comparison is 'clean' in the sense that a reference dataset without the impact of the eclipse has been generated. No such reference can be generated for observations, and various surrogate references must be used. Figure 7 can be compared with Fig. 4 of [19], which shows the difference between the minimum temperature during the eclipse and the maximum prior. As stated in the paper, this is likely to be a conservative estimate as it neglects the diurnal increase in temperature which would have occurred. Nevertheless, the general pattern is in agreement, with the largest impacts in the cloud-free region over Wales, Central England. The modelled differences are generally higher, and discussion below (Sec. (b)) confirms that this can be explained by the method used by [19].

An alternative reference, essentially the same as used in this paper, i.e. the UKV forecast, is used by [20]. This has the drawback of including forecast error but does take account of the diurnal cycle. Fig. 5(c) of [20] is probably the closest comparison with Fig. 7.

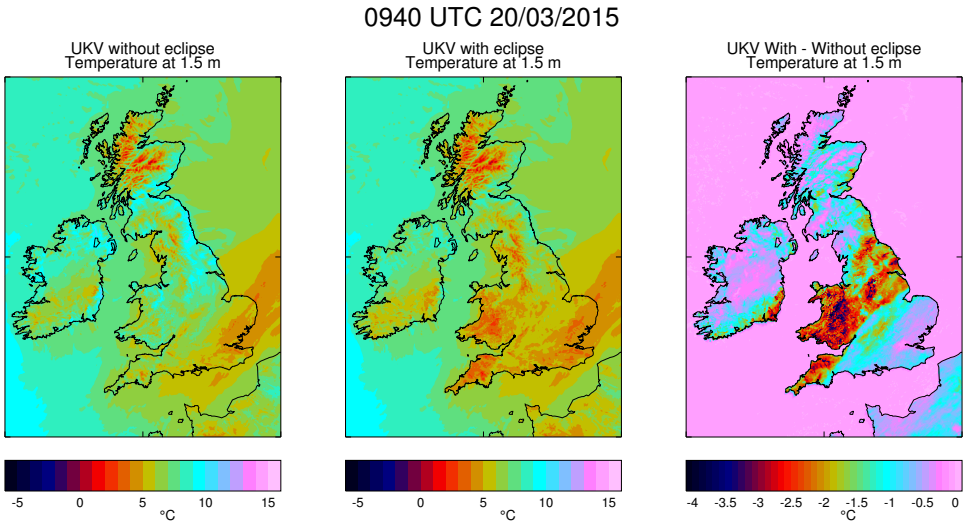

Figure 7. Map of screen temperature at 0940 UTC, left to right, without eclipse, with eclipse and difference

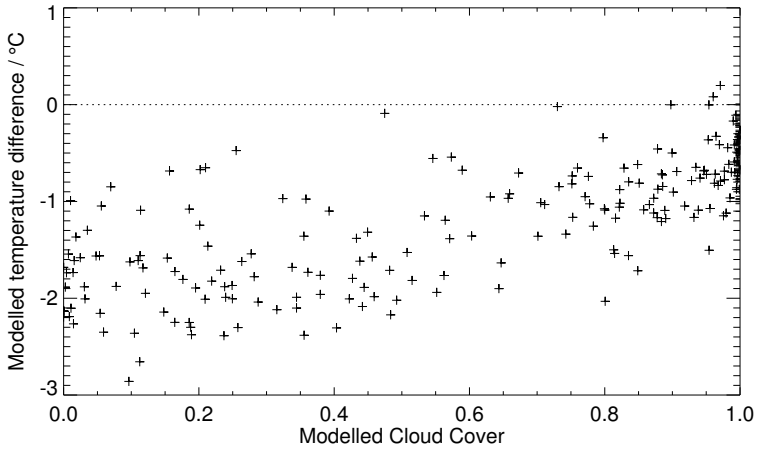

Figure 8. Scatter plot of screen temperature difference (between with and without eclipse) at 1000 UTC vs modelled total cloud cover at land synoptic observation sites.

Unsurprisingly, all of the studies of this event cited show maximum impact on near-surface temperature in the cloud free region. Figure 8 shows the relationship between modelled temperature difference and total cloud cover at 1000 UTC at a set of sites routinely monitored by

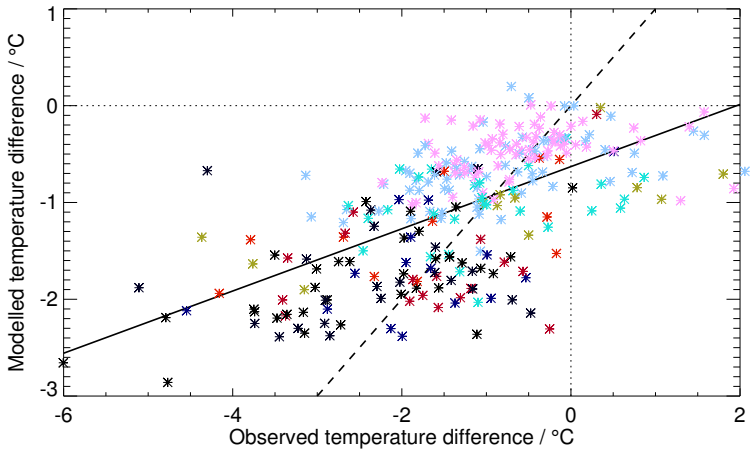

Figure 9. Scatter plot of modelled temperature deficit against observed temperature deficit, colour coded by modelled cloud cover at 1000 UTC. The dashed line is the 1:1 line. The solid line is the line arrived at by regressing modelled temperature deficit against observed temperature deficit.

the Met Office (available from the Met Office Integrated Data Archive System (MIDAS) database). While this shows considerable scatter, the role of cloud is quite evident, with deficits between 1 and 3 °C at near-zero cloud cover. This may be compared with Fig. 6(a) of [21] and Fig. 6 of [19], which shows the equivalent from observations. The 'observed' temperature anomaly is based upon assumptions about recovery of the near-surface temperature after the eclipse which, it will be shown below, are not justified. Nevertheless, there is clearly considerable similarity between the plots.

Figure 9 shows the observed temperature deficit (i.e. observed screen temperature minus modelled screen temperature without eclipse) plotted against modelled temperature deficit for a number (280) of Met Office observing sites over the UK. The markers are colour-coded by modelled cloud cover. This shows the same trend with cloud cover, and a clear correlation between modelled and observed deficit. The dynamic range of the observed response is somewhat larger than modelled, with a few sites approaching 6 °C. The sites with large deficits are all associated with complex terrain, mainly Wales or the south west peninsula, suggesting that local, orographically-modified flows may enhance the impact. In fact, these sites are those for which the tends to perform least well when forecasting temperature and wind, as even 1.5 km is insufficient to resolve the smaller river valleys, so it is quite likely that some of the observed enhancement is simply forecast error.

A second factor modulates the eclipse response. Careful examination of Fig.7 shows that the largest response is under clear skies in rural locations. Despite being largely cloud free, urban areas such as Birmingham, Nottingham, Derby, Stoke-on-Trent show up clearly as areas with smaller eclipse impact than their surroundings (typically 1 °C). The model includes a simple parametrization of the effect of urban areas on surface exchange [22]. This includes representation of the high thermal inertia produced by the mass of buildings. As a result, the surface responds more slowly to increases in incoming SW after dawn, and, hence, produces less impact when the incoming short wave is briefly interrupted. Clark (2016) [21] suggests a smaller observed eclipse impact in urban areas, but the magnitude of the difference is less than 0.5 °C and not statistically significant. This may be a reflection of the nature of the data used, as few stations are in truly urban environments, but is consistent with the hypothesis that the model under-predicts the eclipse impact in urban areas.

The interruption of vertical turbulent mixing has an impact on the boundary-layer wind profile. The impact on 10 m wind at 0940 UTC over England is shown in Fig. 10. Winds over land were very light (at most a few m s^{-1}). The impact on speed (not shown) is generally very small (a fraction of 1 m s^{-1}). The primary impact is a turning of the wind. In almost all cases, the 10 m wind is turned to the left (backed) with the eclipse present, typically by about 20°. This is consistent with the eclipse delaying the growth of the unstable boundary-layer. The nocturnal stable boundary layer generally has a surface wind substantially backed from the free-stream or geostrophic wind; in a stable boundary layer with constant flux Richardson number, the theoretical surface backing is 60 ° [23]. In practice, these conditions rarely apply, but a substantial backing is expected. The reduces as the CBL develops, so the backing due to the eclipse is consistent with the absence of CBL growth. Other variables have been examined in the model.

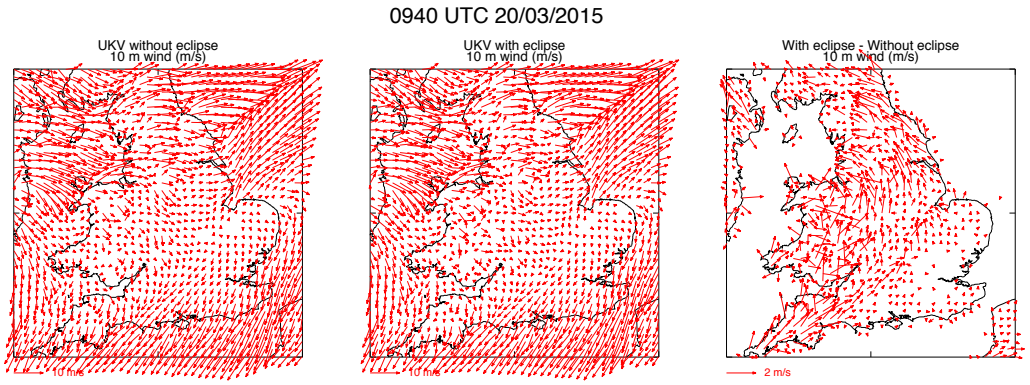

Figure 10. Map of 10 m vector wind at 0940 UTC, left to right, without eclipse and difference

In particular, the surface and mean-sea-level pressure distributions have been examined. While there is an impact of the eclipse, especially around complex terrain, the impact on the meso- or synoptic-scale pressure pattern is a small fraction of a hPa. This is far too small to explain the changes in wind-direction. This is not surprising. Since much of the eclipse shadow falls over the sea, thermal effects on surface pressure driven by surface cooling are expected to be much smaller than they would be over land.

(b) Time History of Eclipse Impact

Though broad behaviours have been identified above, every location is unique in terms of local land-use, wind, cloud cover etc.. Four representative sites for which Met Office near-surface observations are available have been selected to illustrate common behaviours: Hampstead, London; South Farnborough, both with thick cloud cover; Coton in the Elms, South Derbyshire, a rural, central England site with negligible cloud cover in the region which shows most eclipse response over central England in Fig. 7, and a site about 1 km south Lake Vyrnwy, Powys, Wales, in the region which shows most eclipse response over Wales in Fig. 7. Time histories of key variables are shown in Fig. 11.

The model suggests that even the London site shows a small response in surface temperature, which persists into the forecast. The screen-level temperature impact is very small close to maximum eclipse (less than 0.5 °C) during the eclipse, but it grows through the forecast, approaching 0.5 °C at 1200 UTC. From evaluating animations of the spatial pattern it is evident that this is largely due to air with a larger eclipse-impact slowly drifting SE. The observed temperature, when compared with the model, shows a larger response at eclipse time (approaching 1 °C) and apparently recovers around 1200 UTC. It is unlikely that the model provides sufficiently accurate reference here, but it can be said that the observed temperature

shows a distinct minimum of around 0.5 °C. Neither the model nor observations suggest any significant impact on wind.

South Farnborough shows a substantial modelled surface-temperature impact, about 2.5 °C, about 5 minutes after maximum eclipse. A screen temperature deficit of about 0.8 °C grows through the forecast similarly to the London deficit. However any observed impact is very small (there is a hint of a minimum), and the temperature does not substantially increase by 1200. This is very likely related to an under-prediction of cloud optical depth by the model. The model again predicts little impact on wind, though observations show a weakening and veering of the wind after the time of maximum eclipse.

The south Derbyshire site, with maximum temperature impact in the model, shows quite close agreement with the observed screen temperature, with maximum impact about 2.5 °C in screen temperature and more than 6 °C impact on surface temperature. The model suggests there is only extremely small impact on 10 m wind, while the observed wind drops from the already very light 2 m s^{-1} to less than 1 m s^{-1}. The model predicts up to 30° backing of the wind. The absolute direction is not well forecast, which is not surprising given the very low speed, but there is a suggestion of similar or larger backing.

The behaviour at the Welsh site is quite similar in screen temperature, even though the surface temperature impact is smaller. The observed wind speed is even lighter than that modelled, and shows complex behaviour. The wind speed drops to near zero for a 15-minute period after 0945 UTC; this does very roughly correspond to a (less rapid) reduction in the modelled wind speed.

The model is a deterministic model, to the extent that re-runs on the same platform and with the same initial data lead to identical (bit-reproducible) results. Thus, the difference between model runs is exactly that due to the change in forcing caused by the eclipse. However, when compared with observations, in addition to initial condition uncertainty and systematic model error, one has to take into account the upscale growth of small-scale variability not represented in the model. This mainly arises from the fact that the model uses an 'ensemble-mean' boundary-layer parametrization. A true volume-mean would have some turbulent energy at the scales represented by the model. A stochastic representation of this is under development, but was not available for the experiments reported here. However, the main impact is in convective boundary layers (which would be developing in the cloud-free region), leading to 'noise' of order 0.1 °C. On very convective days, this can take several hours to influence the development of, for example, deep convective clouds [25], and, indeed, the forecasts reported here show variations after 12 h or so in the convective cloud developing in the northern part of the domain which are similar to that which would arise from boundary-layer uncertainty alone. However, the differences in temperature over the first few hours are large enough that they can be systematically ascribed to the eclipse forcing change. The same is not true of wind impacts; while the impacts are clearly systematic and consistent with the boundary-layer formulation, they are far to small to be considered to be important when compared with outher sources of variability, such as local orography and surface cover.

(c) Boundary Layer Structure

In the absence of the eclipse, under clear skies, at this time of day, the positive surface sensible heat flux would result in a growing convective boundary layer (CBL). The near-surface temperature depends upon how much air the surface sensible heat flux warms, and hence the initial stable profile. The boundary-layer depth from the model, (strictly, the depth of turbulent mixing) at 0940 UTC is shown in Fig. 12. In the clear region, over flat terrain, the nocturnal stable boundary layer grows in the model to 200-300 m in the absence of the eclipse. With it, convective growth ceases and the depth remains on or below 100 m. Where cloudy, the low-cloud top generally dictates this depth. This is about 600 m over SE England and E. Anglia, deeper to the NW and changes very little with the eclipse.

These behaviours are also illustrated in the time series in Fig. 11. The S Derbyshire site starts with a boundary-layer depth less than 100 m, which grows to about 600 m by 1200 UTC in the

absence of the eclipse. With it, there is a hint of the start of growth just after 0900 UTC, but it soon collapses back to less than 50 m. In contrast to the S Derbyshire site, the modelled boundary layer depth at the mid-Wales site is deep. This seems to be an artefact of the diagnosis procedure, as the boundary layer structure (not shown) is very similar to that at the S Derbyshire site. Nevertheless, it is interesting to note that the diagnosed boundary-layer depth collapses (indicating surface stabilisation) in the with-eclipse simulations at about the time the modelled (and observed) wind speed drops.

The behaviour at the S Derbyshire site is shown in more detail in Figs. 13, 14 and 15. The potential temperature profile shows very classical CBL growth without the eclipse, and quite similar behaviour with the eclipse but delayed. Note that the largest temperature difference in this profile happens about half an hour after peak eclipse. This is later than the surface and very near surface temperatures, reflecting, therefore, the 'inertia' of the boundary layer, rather than sub-surface in determining this delay.

The wind behaviour is complex. A low level jet exists at about 500 m at 0930 UTC. This weakens and rises as the convective boundary layer grows in the absence of the eclipse. With it, this jet develops a second maximum in the stable layer at 200 m, and re-intensifies later at about 600 m. There is only a very shallow layer near the surface of weaker winds, though the layer of backed wind is much more distinct. It is conceivable that discrepancies between modelled and observed wind behaviour is contributed to be the fact that many anemometers are not located at 10 m, and are reports are corrected to 10 m using a relatively simple correction. However, it must be emphasised that, though the flow is weak, there is considerable mesoscale structure in the low-level flow field.

5. Summary and Conclusions

The direct impact of the 20 March 2015 Eclipse on UK weather has been evaluated using simulations performed with a high-resolution state-of-the-art numerical weather forecast model with and without the eclipse. On this occasion, the major impact was surface-driven through changes to surface heat and moisture fluxes. These, in turn, changed the boundary-layer development. In cloud-free areas, the nocturnal stable boundary-layer persisted or quickly re-established during the eclipse. In addition to reduction in surface temperature (7-8 °C) and near-surface air temperature (1-3 °C), near-surface winds were backed, typically by 20 ° relative to the no-eclipse conditions because of the reduced vertical turbulent mixing. Comparison with other studies based upon observations available on the day suggests that these simulated impacts on near-surface temperatures are quite realistic. Impacts on wind speed were small and variable and would have been very difficult to detect. It is likely that they were strongly influenced by local flows promoted by the shallow, stable boundary layer.

Smaller impacts occurred beneath cloud; the depth of mixing remained determined by cloud depth, and a substantial proportion of incoming solar radiation would have been reflected by cloud anyway. However, the impact was enhanced because most of the remaining incoming radiation was driving surface sensible heat flux rather than moisture flux, and the near surface air temperature impact (0.5-1 °C) agrees reasonably well with observations.

The impact of the eclipse was substantially reduced in urban areas due to their large thermal inertia. This contributes, in general, to the nocturnal urban heat island, by delaying the response to incoming solar radiation, but also delays the heating after dawn. The short time-period of the eclipse was such that the model only effectively responded to a fraction of the reduced incoming radiation. Experience from other assessments of the model suggests that this lack of response may be exaggerated [26].

Surface impacts propagated upwards and downstream with time, resulting in a complex pattern of response, though generally near-surface temperature differences persisted for many hours after the eclipse.

Impact on atmospheric pressure fields was insufficient to account for any significant perturbations to the wind field when compared with the direct impacts of surface stress and

boundary-layer mixing. This is primarily because much of the umbra and penumbra was over the sea. The model does not have the capability to predict the direct impact of the reduction in incoming radiation on sea-surface temperature, but it is expected to be negligible. In addition, of course, greater impacts would have been anticipated had the eclipse occurred closer to noon in midsummer.

Data accessibility. Model simulations are available through the University of Reading repository : see Clark, Peter A (2016): MetUM_UKV_eclipse_2015, University of Reading, http://researchdata.reading.ac.uk/id/eprint/51 Met Office surface observations are available from the MIDAS database through the British Atmospheric Data Centre (BADC).

Acknowledgements. Eclipse Predictions by Fred Espenak, NASA's GSFC. The author acknowledges the Met Office for use of the MetUM, initial and boundary data, and observational data. Particular thanks go to Jorge Bornemann and Chloe Eagle for their major contribution to providing real-time forecasts on the day of the eclipse.

References

1 Clayton H. H., 1901, The eclipse cyclone and the diurnal cyclones. *Ann. Astron. Observ. Harvard College*, **43**: 5-22.
2 Aplin K. L., Harrison R. G. 2003 Meteorological effects of the eclipse of 11 August 1999 in cloudy and clear conditions. *Proc. R. Soc. Lond. A* **459**: 353-371. doi:10.1098/rspa.2002.1042
3 Gross P., Hense A., 1999, Effects of a total solar eclipse on the mesoscale atmospheric circulation over Europe - a model experiment. *Meteorol. Atmos. Phys.*, **71**: 229-242. doi:10.1007/s007030050057
4 Anderson R. C., Keefer D. R., 1975, Observation of the temperature and pressure changes during the 30 June 1973 solar eclipse. *J. Atmos. Sci.* **32**: 228-231. doi:10.1175/1520-0469(1975)032<0228:OOTTAP>2.0.CO;2
5 Hanna E., 2000, Meteorological effects of the solar eclipse of 11 August 1999. *Weather* **55**: 430-446
6 Gray, S. L. and Harrison, R. G., 2012, Diagnosing eclipse-induced wind changes. *Proceedings of the Royal Society A: Mathematical, Physical and Engineering Sciences*, **468**: (2143). 1839-1850. ISSN 1364-5021 doi: 10.1098/rspa.2012.0007
7 Prenosil T. 2000 The influence of the 11 August 1999 total solar eclipse on the weather over central Europe. *Meteorol. Z.* **9**: 351-359.
8 Clark, P.A., Roberts, N.M., Lean, H.W., Ballard, S.P. and Charlton-Perez, C., 2015, Convection-permitting models: a step-change in rainfall forecasting, *Meteorol. Appl.* (In press)
9 Cullen, M.J.P., Davies, T., Mawson, M.H., James, J.A., Coulter, S.C. and Malcolm A., 1997 An overview of Numerical Methods for the Next Generation UK NWP and Climate Model Numerical Methods in Atmospheric and Ocean Modelling. In The Andre J.Robert memorial volume. Edited by Charles A Lin, Rene Laprise and Harold Ritchie, Canadian Meteorological and Oceanographic Society, Ottawa, Canada, 425-444
10 Davies, T.; Cullen, M.J.P.; Malcolm, A.J.; Mawson, M.H.; Staniforth, A.; White, A.A.; Wood, N., 2005, A new dynamical core for the Met Office's global and regional modelling of the atmosphere, *Q. J. R. Meteorol. Soc.*, **131**: 1759-1782
11 Essery, R. , Best, M. an Cox, P. 2001, MOSES 2.2 Technical Documentation, Hadley Centre Technical Report No. 30, Met Office Hadley Centre
12 Lock, A.P., Brown, A.R., Bush, M.R., Martin, G.M. and Smith, R.N.B. 2000, A New Boundary Layer Mixing Scheme. Part 1: Scheme Description and Single-Column Model Tests. *Mon. Wea. Rev.*, **128**: 3187-3199.
13 Gregory, D. and Rowntree, P.R. 1990 A Mass Flux Convection Scheme with Representation of Cloud Ensemble Characteristics and Stability-Dependent Closure. *Mon. Wea. Rev.*, **118**: 1483-1506.
14 Wilson, D. R. and Ballard, S. P., 1999. A microphysically based precipitation scheme for the UK Meteorological Office Unified Model., *Q. J. R. Meteorol. Soc.*, **125**: 1607-1636.
15 Rawlins FR, Ballard SP, Bovis KR, Clayton AM, Li D, Inverarity GW, Lorenc AC, Payne TJ. 2007. The Met Office global 4-Dimensional data assimilation system. *Q. J. R. Meteorol. Soc.*, **133**: 347-362.

16 Lorenc AC, Ballard SP, Bell RS, Ingleby NB, Andrews PLF, Barker DM, Bray JR, Clayton AM, Dalby T, Li D, Payne TJ, Saunders FW. 2000. The Met. Office global 3-Dimensional variational data assimilation scheme. *Q. J. R. Meteorol. Soc.*, **126**: 2991-3012.
17 Espanak, F., 2015, http://eclipse.gsfc.nasa.gov/SEpath/SEpath2001/SE2015Mar20Tpath.html
18 Edwards JM, Slingo A. 1996. Studies with a flexible new radiation code. I: Choosing a configuration for a large-scale model. *Q. J. R. Meteorol. Soc.* **122**: 689-719.
19 Hanna, E., Penman, J., JÃşnsson, T., Bigg, G.R., BjÃűrnsson, H., SjÃžrÃřarson, S., Hansen, M.A., Cappelen, J. and Bryant, R.G., 2016, Meteorological effects of the solar eclipse of 20 March 2015 - analysis of UK Met Office automatic weather station data and comparison with AWS data from the Faroes and Iceland *Phil. Trans. R. Soc. A.*, This volume.
20 Gray, S.L. and Harrison, R.G., 2016, Eclipse-induced wind changes over the British Isles on the 20 March 2015, *Phil. Trans. R. Soc. A.*, This volume.
21 Clark, M.R., 2016, On the variability of near-surface screen temperature anomalies in the 20 March 2015 solar eclipse, *Phil. Trans. R. Soc. A.*, This volume.
22 Best M.J., 2005: Representing urban areas within operational numerical weather prediction models., *Boundary-Layer Meteor.*, **114**: 91-109.
23 Garratt J. R., 1994, The atmospheric boundary layer. Cambridge, UK: Cambridge University Press.
24 Burt, S., 2016, Meteorological responses in the atmospheric boundary layer over southern England to the deep partial eclipse of 20 March 2015, *Phil. Trans. R. Soc. A.*, This volume.
25 Perturbation growth at the convective scale for CSIP IOP18, 2010, G. Leoncini, R.S. Plant, S.L. Gray and P.A. Clark, *Quart. J. Roy. Meteorol. Soc.*, **136**: 653-670.
26 Porson, A., Clark, P. A., Harman, I. N., Best, M. J. and Belcher, S. (2010) Implementation of a new urban energy budget scheme into MetUM. Part II: Validation against observations and model intercomparison. *Quarterly Journal of the Royal Meteorological Society*, **136**(651): 1530-1542. ISSN 1477-870X doi: 10.1002/qj.572

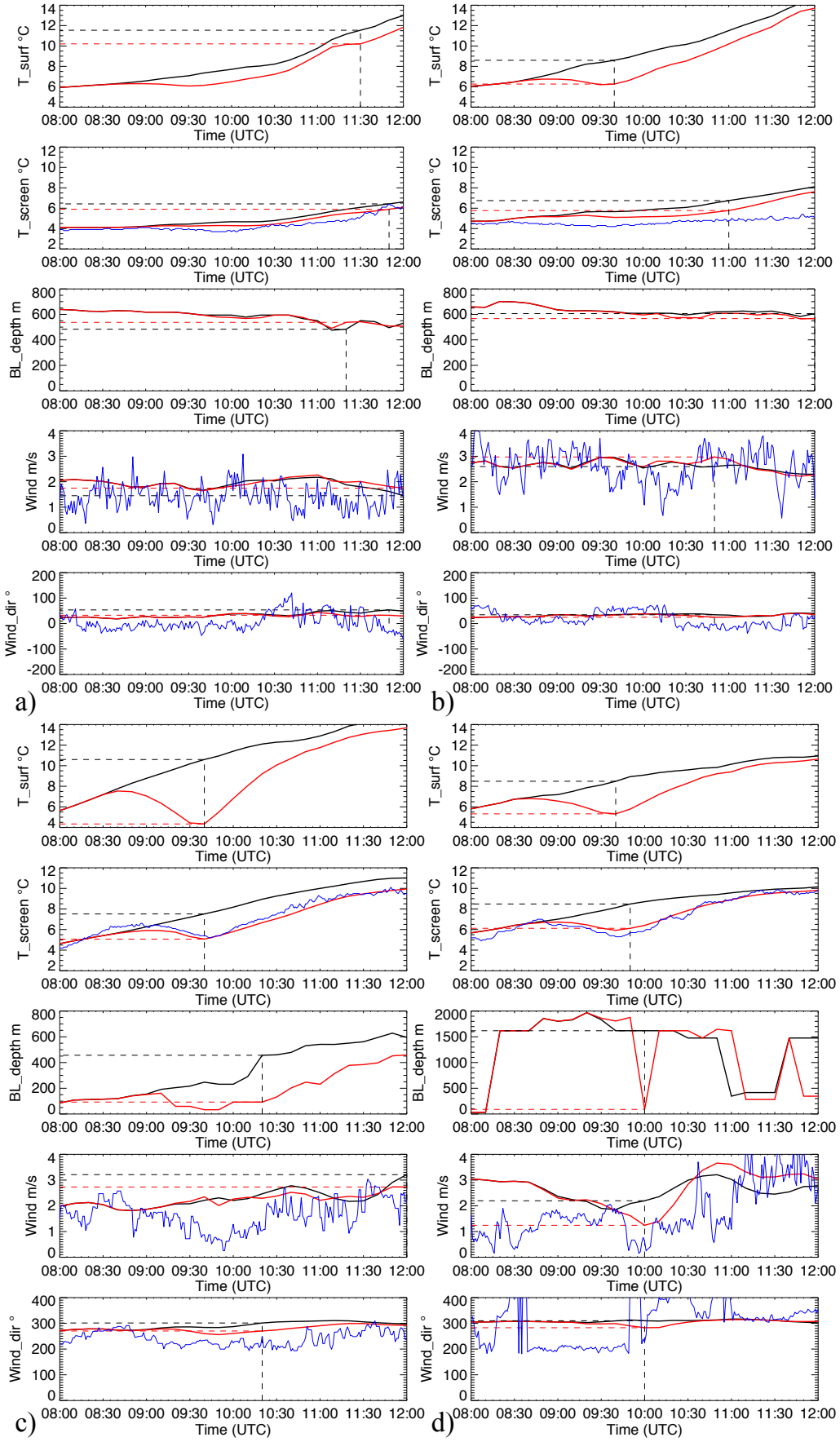

Figure 11. Time series of (top to bottom) surface temperature, screen temperature, boundary-layer depth, without eclipse (black), and with eclipse (red) at (a) Hampstead, London (51.56009 °N, 0.17839 °W) (b) South Farnborough, East Hampshire (51.27944 °N, 0.77107 °W), (c) Coton in the Elms, South Derbyshire (52.73673 °N, 1.6396 °W) and (d) Lake Vyrnwy, Powys, Wales (52.75701 °N, 3.46411 °W). Observed screen temperatures, wind speed and direction at 10 m are shown as blue lines.

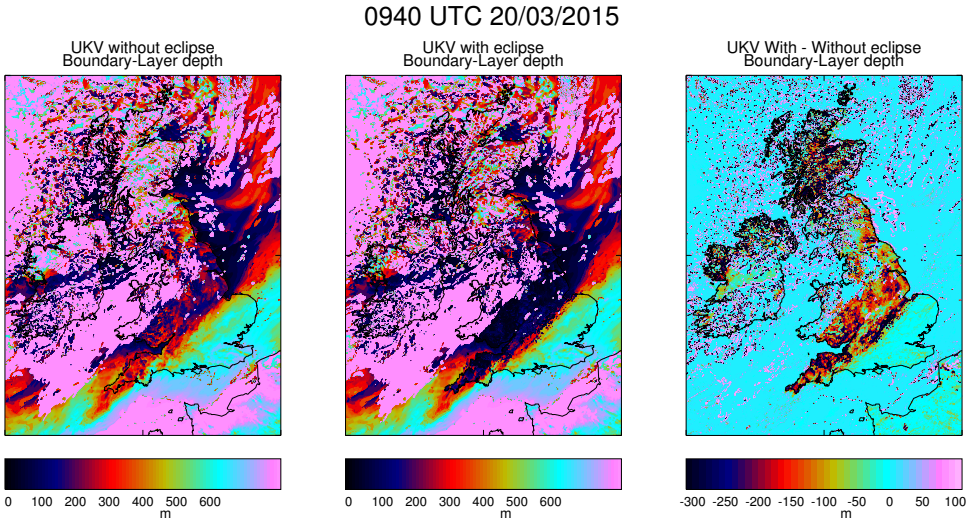

Figure 12. Map of boundary-layer depth at 0940 UTC, left to right, without eclipse, with eclipse and difference

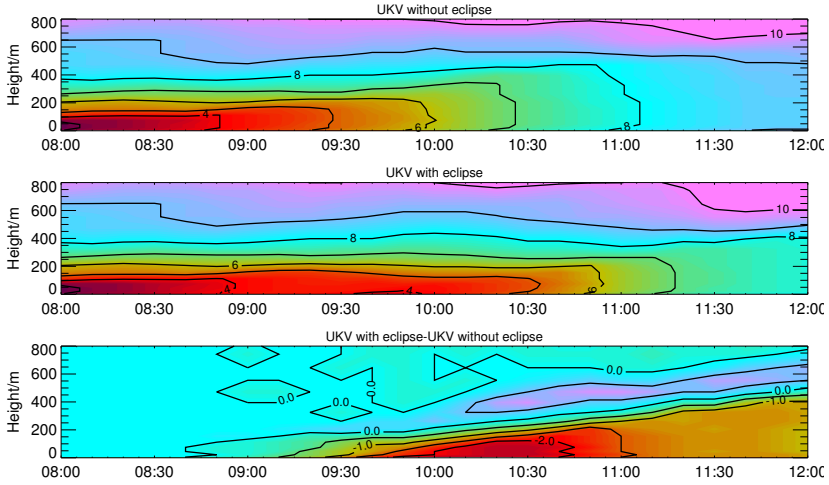

Figure 13. Vertical time/height profiles of potential temperature at Coton in the Elms, South Derbyshire, without eclipse (top), with eclipse (middle) and difference (bottom)

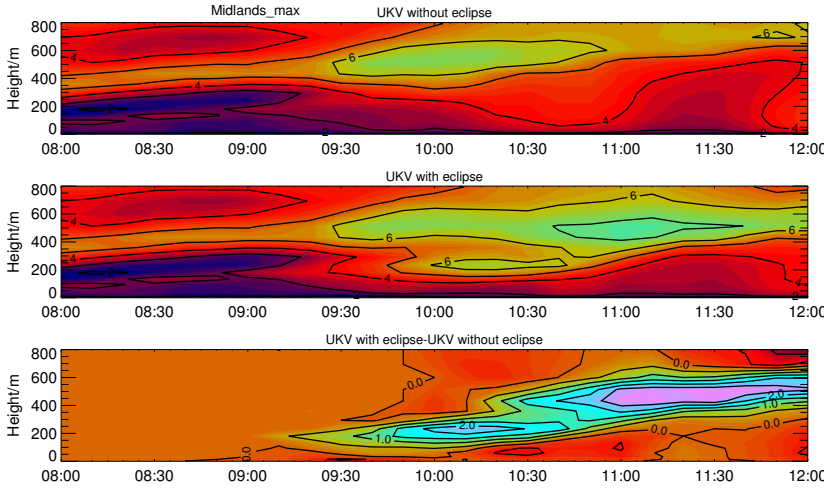

Figure 14. Vertical time/height profiles of wind speed at Coton in the Elms, South Derbyshire, without eclipse (top), with eclipse (middle) and difference (bottom)

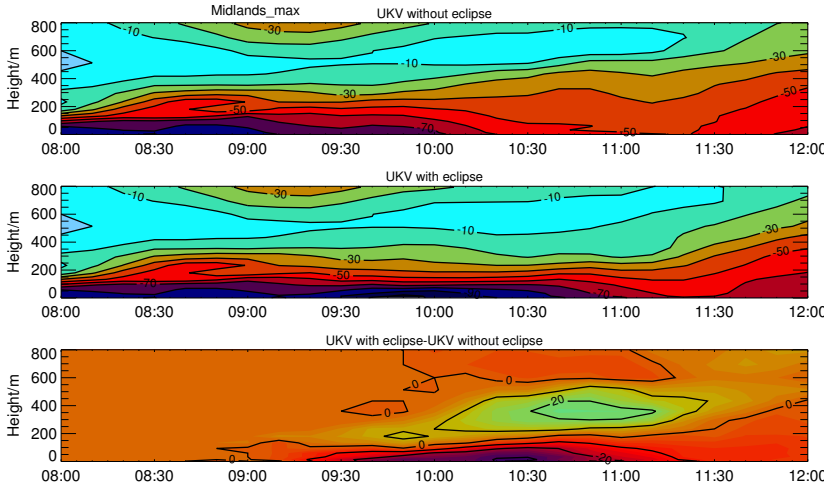

Figure 15. Vertical time/height profiles of wind direction at Coton in the Elms, South Derbyshire, without eclipse (top), with eclipse (middle) and difference (bottom)